Mixed-valence state of the rare-earth compounds YbXCu$_4$ (X = Mg, Cd, In, and Sn): Magnetic susceptibility, x-ray diffraction, and x-ray absorption spectroscopy investigations

Hiroaki Anzai [⬤],[1,*] Suzuna Ishihara,[1] Hiroto Shiono,[1] Kohei Morikawa,[1] Toshiaki Iwazumi,[1] Hitoshi Sato,[2]
Tao Zhuang,[3] Keisuke T. Matsumoto,[3] and Koichi Hiraoka[3,†]

[1]*Graduate School of Engineering, Osaka Prefecture University, Sakai 599-8531, Japan*
[2]*Hiroshima Synchrotron Radiation Center, Hiroshima University, Higashi-Hiroshima 739-0046, Japan*
[3]*Graduate School of Science and Engineering, Ehime University, Matsuyama, Ehime 790-8577, Japan*

We report an investigation on the mixed-valence state for YbXCu$_4$ compounds with X = Mg, Cd, In, and Sn. The x-ray diffraction measurements on X = Sn have revealed a cubic AuBe$_5$-type structure with the lattice constant $a = 7.123$ Å. The Kondo temperature of X = Sn is determined to be $T_K = 503$ K from the value of magnetic susceptibility. We have observed a mixing of the Yb^{2+} and Yb^{3+} electronic states from the x-ray absorption spectra at 300 K and a change in their relative intensities with varying X atoms, indicating a different degree of valence mixing in YbXCu$_4$. Our data clearly exhibit correlations among the energy of the Yb^{3+} peak, the degree of valence mixing, and the Kondo temperature. These results suggest that the $5p$ electrons of X atoms play an important role in the mixed-valence state of YbXCu$_4$ by controlling the number of the Yb $4f$ electrons.

I. INTRODUCTION

A mixed-valence state in rare-earth compounds is one of the most intriguing subjects. In particular, YbInCu$_4$ has attracted considerable interest, because it exhibits a first-order valence transition between $4f^{13}$ (trivalent) and $4f^{14}$ (divalent) electron configurations at $T_V = 42$ K [1,2]. The mean valence of Yb ions determined by the Mössbauer spectroscopy measurements changes from $z \sim 2.9$ for $T > T_V$ to $z \sim 2.8$ for $T < T_V$ [2]. Concomitantly, the temperature dependences of the lattice volume, electric resistivity, and magnetic susceptibility show a discontinuity at T_V [2,3]. A driving force for the valence transition is considered to be the hybridization between conduction and $4f$ electrons (c-f hybridization). The Kondo temperature T_K, which is a measure of the hybridization strength, varies from $T_K \sim 25$ K in the high-temperature phase to $T_K \sim 400$ K in the low-temperature phase [4]. It has been suggested that conduction electrons at the Cu and In sites mediate the electron transfer in $4f$ orbitals [5–7]. Hence studies in terms of the conduction electrons are required to clarify the driving factors for the valence transition in YbInCu$_4$.

The In-substituted compounds YbXCu$_4$ (X = Mg, Cd, Ag, Au, Zn, etc.) provide us with a unique opportunity to understand the mixed-valence state. First, these compounds crystallize in the same AuBe$_5$-type (C15b) structure as YbInCu$_4$ shown in Fig. 1(a), and the Kondo temperature changes with varying X atoms [8,9]. For instance, the Kondo temperatures calculated from Wilson's formula, $T_K = 1.29T_0$, are $T_K \sim 1109$ K for X = Mg and $T_K \sim 287$ K for X = Cd, where T_0

is the characteristic temperature determined by the value of zero-temperature susceptibility [9–13]. Such a large variation in T_K leads to a detectable change in electronic structures derived from the effect of hybridization. We have successfully grown single crystals of YbSnCu$_4$, but the fundamental physical parameters such as lattice constant, Kondo temperature, and Yb valence have remained unclear. It is thus important to revisit the electronic structures in the series of YbXCu$_4$ compounds under the same experimental conditions. Second, only the YbInCu$_4$ exhibits the valence transition [9–11]. For X atoms in the fifth periodic elements, the nominal valence electron configurations of Cd, In, and Sn are respectively $5s^25p^0$, $5s^25p^1$, and $5s^25p^2$, implying its relevance to the emergence of the valence transition. Therefore, the study of the electronic states as a function of X atom will provide valuable information on the valence transition.

X-ray absorption spectroscopy (XAS) is a bulk probe to measure both unoccupied and occupied electronic states with elemental and orbital selectivity. The energy and intensity of the absorption edge reflect the valence state. A number of XAS experiments have been performed on YbInCu$_4$, and they revealed the mixed-valence state of $4f$ electron configurations from the spectra of Yb L_{III} edge [14–17]. In contrast, the XAS spectra for X = Mg, Cd, and Sn have been rarely reported thus far.

Here, we present a study of the mixed-valence state in YbXCu$_4$ (X = Mg, Cd, In, and Sn). The lattice constant and Kondo temperature of X = Sn are respectively estimated from x-ray diffraction and magnetic susceptibility measurements. With improved data quality, the obvious material dependence of the peak intensity is identified in the Yb L_{III} XAS spectra at 300 K. Quantifying the parameters of the Yb^{2+} and Yb^{3+} components, we show the correlations among the energy of the Yb^{3+} peak, the degree of valence mixing, and the Kondo

*anzai@pe.osakafu-u.ac.jp
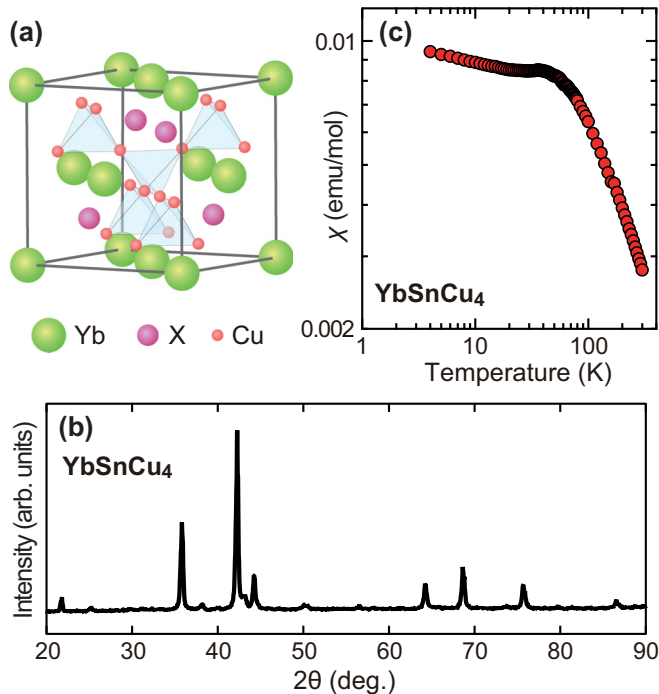†hiraoka.koichi.mk@ehime-u.ac.jp

FIG. 1. (a) Schematic crystal structure of YbXCu$_4$ with AuBe$_5$-type cubic lattice. (b) The x-ray diffraction pattern of the single crystal YbSnCu$_4$ at $T = 300$ K. The diffraction lines are indexed on the basis of the AuBe$_5$-type cubic structure with a lattice constant $a = 7.123$ Å. (c) Magnetic susceptibility $\chi(T)$ of YbSnCu$_4$ in a magnetic field of 10 kOe. The data are plotted on logarithmic scales.

FIG. 2. XAS spectra of YbXCu$_4$ (X = Mg, Cd, In, and Sn) measured at $T = 300$ K. The original data for X = Cd and In are reported in Ref. [17]. (a) The XAS spectra at the Yb L_{III} edge. The spectra of Yb$_2$O$_3$ are also shown as a reference for the $4f^{13}$ electron configurations of Yb ions. (b) The spectra at the Cu K edge, together with the spectra of Cu$_2$O as a reference material for the $3d^{10}$ electron configurations.

temperature. We propose that the low non-$4f$ density of states near the Fermi level (E_{F}) and their substantial energy shift plays an important role in the valence transition of YbInCu$_4$.

High-quality single crystals of YbXCu$_4$ with X = Mg, Cd, In, and Sn were synthesized by the flux method [18–20]. The reference samples of Yb$_2$O$_3$ and Cu$_2$O were prepared using commercially available powders. The x-ray diffraction measurements were preformed at $T = 300$ K on a powder of crushed single crystals YbSnCu$_4$. The lattice parameters were calculated using the peak positions by least-square calculations. The magnetic susceptibility measurements of the X = Sn compound were performed with a superconducting quantum interference device (SQUID) magnetometer. The XAS experiments with synchrotron radiation were performed at beamline 7C of the Photon Factory. The spectra were collected in the transmission mode using ionization chambers at $T = 300$ K. The energy resolution was ~1 eV at the Yb L_{III} edge. The energy was calibrated at the preedge peak observed in the Cu K edge XAS spectrum of the Cu foil.

II. RESULTS AND DISCUSSION

Figure 1(b) shows the x-ray diffraction pattern of YbSnCu$_4$. The pattern can be indexed on the AuBe$_5$-type cubic structure shown in Fig. 1(a). Thus all the samples (X = Mg, Cd, In, and Sn) exhibit the same structure at $T = 300$ K. The lattice constant is estimated to be $a = 7.123$ Å from the Rietveld refinements.
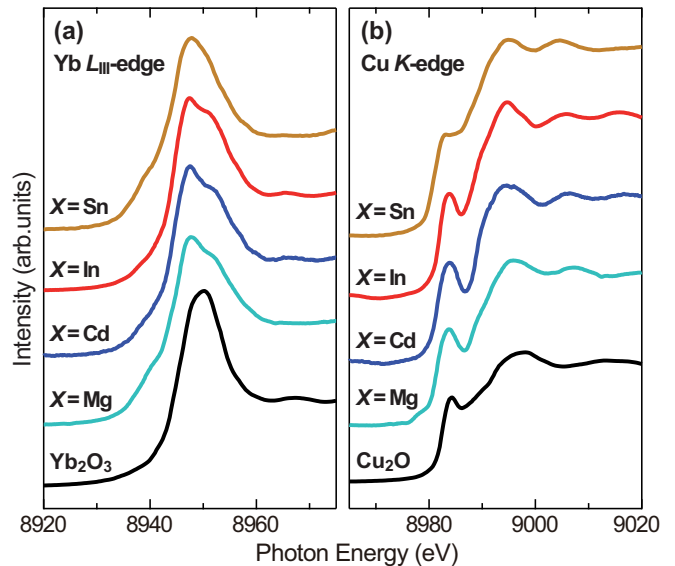
The temperature dependence of the magnetic susceptibility $\chi(T)$ of YbSnCu$_4$ is shown in Fig. 1(c) on a logarithmic scale. The susceptibility increases with decreasing temperature and exhibits a broad peak at $T \sim 40$ K, which is known to be a characteristic of mixed-valence compounds [9,10]. Then, $\chi(T)$ increases below $T \sim 20$ K, possibly owing to the presence of impurity phases. This upturn at low temperatures is small compared to the data reported in Ref. [9]. A local minimum of the susceptibility is estimated to be $\chi(25) \sim 8.45 \times 10^{-3}$ emu/mol.

The ratio $\chi(T)/\chi(0)$ is a universal scaling with respect to T/T_0 [12]. This universality is associated with the Kondo temperature through Wilson's formula [13]. We have applied the value at the local minimum $\chi(25)$ to the zero-temperature susceptibility $\chi(0)$ and evaluated the Kondo temperature of YbSnCu$_4$ as $T_{\mathrm{K}} = 503$ K.

Figure 2(a) shows Yb L_{III}-edge XAS spectra, which are derived from the electric dipole transition from the Yb $2p_{3/2}$ to Yb $5d$ unoccupied states. The spectra for X = Mg and Sn are compared with those for X = In and Cd reported in Ref. [17]. We also plot the spectrum of Yb$_2$O$_3$ as a standard for trivalent Yb ions. A well-defined absorption peak is observed at $h\nu \sim 8950$ eV in common and is thus assigned to the Yb^{3+} state. The doublet peaks at 8947 and 8952 eV originate from the energy separation of the Yb $5d$ unoccupied density of states [21–23].

For X = Mg, Cd, In, and Sn compounds, a shoulder is observed at ~8940 eV on the low-energy side of the Yb^{3+} peak, as shown in Fig. 2(a). This shoulder is attributed to the L_{III} transitions of the Yb^{2+} electronic state [14–16]. Therefore, the $4f$-electron occupancy of YbXCu$_4$ consists of mixing between the divalent and trivalent states at 300 K [9–11]. It
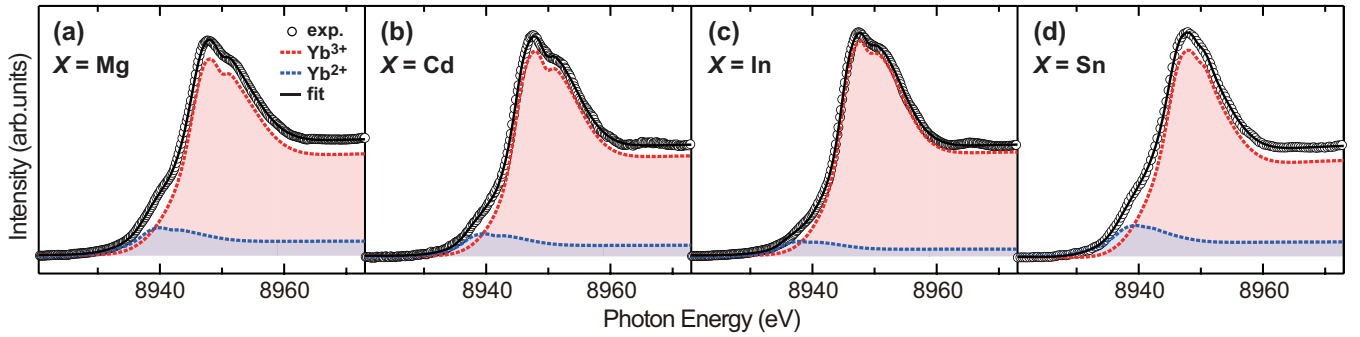
FIG. 3. Fitting results for the Yb L_{III} XAS spectra of YbXCu$_4$. Figures are arranged from left to right in order of increasing electron number of X atoms: (a) $X = $ Mg, (b) $X = $ Cd, (c) $X = $ In, and (d) $X = $ Sn. Open circles are the Yb L_{III} XAS spectra from the same data set as in Fig. 2(a). The black curves represent the results of the fitting analysis. The contributions of the Yb^{2+} and Yb^{3+} components are shown by the dashed blue and red lines, respectively.

is noteworthy that the intensity of the shoulder changes with varying X atoms, implying a change in the degree of valence mixing in YbXCu$_4$.

In Fig. 2(b), we show the Cu K-edge XAS spectra, together with the spectra of Cu$_2$O as a reference material for the $3d^{10}$ electron configurations. A preedge peak and a large absorption peak are clearly observed at $h\nu \sim 8984$ and 8995 eV, respectively. Their energy positions coincide with the peak energies for Cu$_2$O, indicating that the electron configuration at the Cu site of YbXCu$_4$ is in the $3d^{10}$ electronic state as a closed shell. This is in agreement with the results that the satellite peak is not observed in the photoemission spectra of Cu $2p$ orbitals [6,7]. Hence the electrons at the Cu site are less sensitive to varying X atoms than those at the Yb site, as seen from Figs. 2(a) and 2(b).

To quantify the parameters of the Yb^{2+} and Yb^{3+} components, we have performed a fitting analysis of the Yb L_{III} XAS spectra with phenomenological functions [2,14]. Two Lorentzians are applied for each edge in accordance with the observation of doublet peaks at 8947 and 8952 eV. The parameters of the doublet peaks, such as the energy splitting, the peak intensity ratio, and the peak width ratio are fixed for the Yb^{2+} and Yb^{3+} components. The fitting function includes an arctangent background as an incoherent spectral weight. As shown by thick black curves in Figs. 3(a)–3(d), the result of this procedure satisfactorily tracks the shoulder at ~ 8940 eV and the doublet peaks in the Yb^{3+} component.

In Figs. 4(a) and 4(b), we show the energy of the Yb^{3+} peak and the energy difference between the Yb^{3+} peak and the preedge Cu peak, respectively. The horizontal axis is arranged from left to right in order of increasing electron number of X atoms. An energy shift of the Yb^{3+} peak is detected. Specifically, the Yb^{3+} peak for $X = $ In is located at the lowest energy position, and the peaks for $X = $ Mg, Cd, and Sn are shifted to the high-energy side by ~ 0.76, ~ 0.31, and ~ 0.67 eV, respectively.

The Yb valence can be evaluated from the formula $z = 2 + [I_3/(I_2 + I_3)]$, where I_2 and I_3 are the integrated intensities of the Yb^{2+} and Yb^{3+} components, respectively [2,14]. As shown by red circles in Fig. 4(c), z at 300 K increases from $X = $ Mg, to Cd, and to In, and then decreases at $X = $ Sn. The X-dependent behavior of the Yb valence indicates a different degree of the mixed-valence state in YbXCu$_4$. We

note that the values of z for $X = $ In and Sn are consistent with those obtained from XAS and photoemission spectroscopy measurements [2,7,14,15]. On the other hand, the values for $X = $ Mg and Cd deviate from the results reported by Sarrao et al [9]. This discrepancy may arise due to an inadequate sample size and/or quality. Indeed, the temperature dependences of the magnetic susceptibility in the data set of Ref. [9] are strongly deformed at low temperatures, compared to the typical data shown in Fig. 1(c).

The Kondo temperature T_K is also plotted by blue squares in Fig. 4(c). Significantly, T_K is anticorrelated with z as a
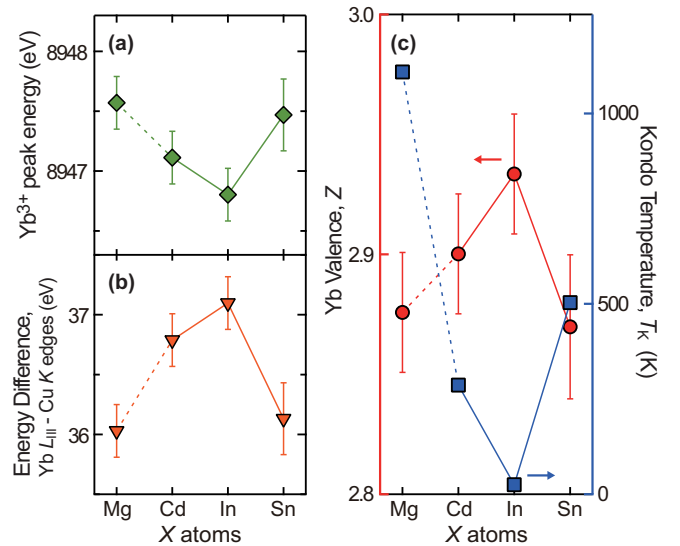

FIG. 4. Parameters extracted from the fitting analysis. The horizontal axis is arranged from left to right in order of increasing electron number of X atoms. (a) The energy of the Yb^{3+} absorption peak. (b) The energy difference between the Yb^{3+} peak and the preedge Cu peak. (c) X dependence of the Yb valence z at $T = 300$ K shown by red circles on left axis. The Kondo temperature T_K is also plotted by blue squares on the right axis. For $X = $ Mg and Cd, T_K is calculated from the Wilson's formula, $T_K = 1.29 T_0$, using the characteristic temperature T_0 reported in Ref. [9]. For $X = $ In, we adopted the Kondo temperature in the high-temperature phase [4]. The data for $X = $ Sn originate from the magnetic susceptibility in Fig. 1(c).

function of X atom. This behavior can be qualitatively explained by the change in carrier density at E_F. Previous measurements of Hall coefficients have revealed that the Fermi level for the high-temperature phase of YbInCu$_4$ lies in the low density of states (quasigap) [24,25]. Such a semimetallic state has a small contribution to the interplay between the conduction and $4f$ electrons, resulting in the weak hybridization of $T_K \sim 25$ K [4]. Thus the Yb ions for $X =$ In remain the nearly trivalent state with one hole in the $4f$ orbitals. The $X =$ Mg and Cd compounds, in contrast, exhibit a metallic behavior with healthy density of states [24]. The enhanced carrier density is available to mediate the c-f hybridization. This is consistent with the recovery of the strong hybridization strength at $X =$ Mg and Cd. The Yb $4f$ hole states are partially occupied by the conduction electrons, and consequently the Yb valence decreases toward the divalent state, as shown in Fig. 4(c).

The change in carrier density at E_F may be understood as a consequence of a rigid shift of the chemical potential. The band structure calculations show that the non-$4f$ density of states are nearly identical for YbXCu$_4$, and they exhibit a rigid-band-like shift with varying X atoms [21–23]. The energy shift of the conduction bands pushes the quasigap away from the Fermi energy. The magnitude of the quasigap $0.5 \sim 1$ eV corresponds to the shift amount of the Yb^{3+} peak shown in Fig. 4(a) [24,25]. Therefore, the number of the Yb $4f$ electrons is considered to be controlled by the $5p$ electrons of X atoms along with the rigid-band-like shift of the conduction bands.

On the other hand, a simple picture of the chemical potential shift cannot be fully accounted for the energy shift of the Yb^{3+} peak. A similar observation has been reported previously on the Cu $2p_{3/2}$ photoemission spectra of YbXCu$_4$ [7]. We note here that the XAS spectra of the Yb L_{III} edge reflect mainly the unoccupied Yb $5d$ states. The hybridization between the In $5p$ and Yb $4f$ states induces heavy quasiparticles and reconstructs the band structure around E_F [26]. It is assumed that the renormalized bands partially pin the Yb $5d$ states to the Fermi level [25], and the position of E_F for $X =$ In deviates from the simple chemical trend. Further investigations such as theoretical calculations are required for the better and quantitative understanding of the nonmonotonic energy shift of the absorption peak.

Next, we discuss the emergence of the valence transition in YbXCu$_4$ among the X atoms in fifth periodic elements. The lattice constants of $X =$ Cd, In, and Sn are respectively 7.135 Å, 7.158 Å, and 7.123 Å [9], indicating a volume dependence of both the Yb valence and the Kondo temperature, as

shown in Fig. 4(c). Thus the unit cell volume can be associated with the strength of the c-f hybridization, similar to the Kondo volume collapse model for the cerium α-γ transition [27]. It has been reported from high-energy x-ray diffraction measurement that the crystallographic symmetry of YbInCu$_4$ changes from a cubic structure to a tetragonal structure at T_V [16]. The enhancement of the unit cell volume implies a large entropy remaining above T_V. We consider that the volume effect on the structural phase transition plays an important role for the valence transition in YbInCu$_4$.

Another clue to the origin of the valence transition is the position of the Fermi level near the quasigap region [24]. Recent resonant inelastic x-ray scattering measurements have revealed an energy shift of itinerant Yb $5d$ states and an increase in the density of states at E_F below T_V [25]. This is analogous to what is observed with varying X atoms, as shown in Figs. 4(a)–4(c). The substantial energy shift of the conduction bands at T_V entails a change in the energy and momentum region where the $4f$ states and conduction bands are interacting [26]. Such an energy shift may originate from the structural phase transition in YbInCu$_4$ [16].

III. CONCLUSION

The mixed-valence state of YbXCu$_4$ compounds has been investigated by x-ray diffraction, magnetic susceptibility, and synchrotron radiation XAS measurements. We have established that the $X =$ Sn compound crystallizes in the cubic AuBe$_5$-type structure with the lattice constant $a = 7.123$ Å and has a Kondo temperature of $T_K = 503$ K. The relative intensity of the Yb^{2+} and Yb^{3+} states in the Yb L_{III}-edge XAS spectra showed a material dependence. A remarkable observation is a correlative behavior among the energy shift of the Yb^{3+} peak, the degree of valence mixing, and the Kondo temperature. This finding provides evidence that the $5p$ electrons of X atoms control the occupancy of the Yb $4f$ electrons along with the rigid-band-like shift of the conduction bands. We suggest that the c-f hybridization near the quasigap and the substantial energy shift of the conduction bands should be incorporated into scenarios of the valence transition in YbInCu$_4$.

[1] I. Felner and I. Nowik, First-order valence phase transition in cubic Yb$_x$In$_{1-x}$Cu$_2$, Phys. Rev. B **33**, 617 (1986).

[2] I. Felner, I. Nowik, D. Vaknin, U. Potzel, J. Moser, G. M. Kalvius, G. Wortmann, G. Schmiester, G. Hilscher, E. Gratz, C. Schmitzer, N. Pillmayr, K. G. Prasad, H. de Waard, and H. Pinto, Ytterbium valence phase transition in Yb$_x$In$_{1-x}$Cu$_2$, Phys. Rev. B **35**, 6956 (1987).

[3] J. L. Sarrao, C. D. Immer, C. L. Benton, Z. Fisk, J. M. Lawrence, D. Mandrus and J. D. Thompson, Evolution from

first-order valence transition to heavy-fermion behavior in YbIn$_{1-x}$Ag$_x$Cu$_4$, Phys. Rev. B **54**, 12207 (1996).

[4] J. M. Lawrence, S. M. Shapiro, J. L. Sarrao, and Z. Fisk, Inelastic neutron scattering in single-crystal YbInCu$_4$, Phys. Rev. B **55**, 14467 (1997).

[5] K. Yoshikawa, H. Sato, M. Arita, Y. Takeda, K. Hiraoka, K. Kojima, K. Tsuji, H. Namatame, and M. Taniguchi, Low-energy excited photoemission study of the valence transition of YbInCu$_4$, Phys. Rev. B **72**, 165106 (2005).

[6] Y. Utsumi, H. Sato, H. Kurihara, H. Maso, K. Hiraoka, K. Kojima, K. Tobimatsu, T. Ohkochi, S. Fujimori, Y. Takeda, Y. Saitoh, K. Mimura, S. Ueda, Y. Yamashita, H. Yoshikawa, K. Kobayashi, T. Oguchi, K. Shimada, H. Namatame, and M. Taniguchi, Conduction-band electronic states of YbInCu$_4$ studied by photoemission and soft x-ray absorption spectroscopies, Phys. Rev. B **84**, 115143 (2011).

[7] Y. Utsumi, H. Sato, K. Tobimatsu, H. Maso, K. Hiraoka, K. Kojima, K. Mimura, S. Ueda, Y. Yamashita, H. Yoshikawa, K. Kobayashi, K. Shimada, H. Namatame, and M. Taniguchi, X-dependent electronic structure of YbXCu$_4$ (X = Cd, In, Sn) investigated by hard x-ray photoemission spectroscopy, J. Electron Spectrosc. Relat. Phenom. **184**, 203 (2011).

[8] E. Bauer, Anomalous properties of Ce-Cu- and Yb-Cu-based compounds, Adv. Phys. **40**, 417 (1991).

[9] J. L. Sarrao, C. D. Immer, Z. Fisk, C. H. Booth, E. Figueroa, J. M. Lawrence, R. Modler, A. L. Cornelius, M. F. Hundley, G. H. Kwei, J. D. Thompson, and F. Bridges, Physical properties of YbXCu$_4$ (X = Ag, Au, Cd, Mg, Tl, and Zn) compounds, Phys. Rev. B **59**, 6855 (1999).

[10] T. Koyama, M. Matsumoto, T. Tanaka, H. Ishida, T. Mito, and S. Wada, Physical properties of the Kondo compounds YbXCu$_4$ (X = Au, Ag, In, Cd, Tl, and Mg) probed by ^{63}Cu NMR, Phys. Rev. B **66**, 014420 (2002).

[11] A. V. Golubkov, L. S. ParfenÕeva, I. A. Smirnov, H. Misiorek, J. Mucha, and A. Jezowski, Thermal conductivity of the YbMgCu$_4$ "Light" heavy-fermion system, Phys. Solid State **49**, 2038 (2007).

[12] V. T. Rajan, Magnetic Susceptibility and Specific Heat of the Coqblin-Schrieffer Model, Phys. Rev. Lett. **51**, 308 (1983).

[13] N. Andrei and J. H. Lowenstein, Scales and Scaling in the Kondo Model, Phys. Rev. Lett. **46**, 356 (1981).

[14] Y. H. Matsuda, T. Inami, K. Ohwada, Y. Murata, H. Nojiri, Y. Murakmi, H. Ohta, W. Zhang, and K. Yoshimura, High-magnetic-field x-ray absorption spectroscopy of field-induced valence transition in YbInCu$_4$, J. Phys. Soc. Jpn. **76**, 034702 (2007).

[15] L. Moreschini, C. Dallera, J. J. Joyce, J. L. Sarrao, E. D. Bauer, V. Fritsch, S. Bobev, E. Carpene, S. Huotari, G. Vankó, G. Monaco, P. Lacovig, G. Panaccione, A. Fondacaro, G. Paolicelli, P. Torelli, and M. Grioni, Comparison of bulk-sensitive spectroscopic probes of Yb valence in Kondo systems, Phys. Rev. B **75**, 035113 (2007).

[16] S. Tsutsui, K. Sugimoto, R. Tsunoda, Y. Hirose, T. Mito, R. Settai, and M. Mizumaki, First-order structural change accompanied by Yb valence transition in YbInCu$_4$, J. Phys. Soc. Jpn. **85**, 063602 (2016).

[17] H. Anzai, S. Ishihara, H. Shiono, K. Mimura, T. Iwazumi, H. Sato, T. Zhuang, K. T. Matsumoto, and K. Hiraoka, in *Proceedings of the 13th International Conference on Synchrotron Radiation Instrumentation – SRI2018*, edited by S. Gwo, D.-J. Huang, and D.-H. Wei, AIP Conf. Proc. No. 2054 (AIP, New York, 2019), p. 040006.

[18] K. Hiraoka K. Kojima, T. Hihara, and T. Shinohara, NMR study of YbCdCu$_4$ and YbTlCu$_4$, J. Magn. Magn. Mater. **140–144**, 1243 (1995).

[19] K. Hiraoka, K. Murakami, S. Tomiyoshi, T. Hihara, T. Shinohara, and K. Kojima, ^{63}Cu NQR and ^{113}Cd NMR studies of YbMCu$_4$ (M = In, Cd), Physica B (Amsterdam) **281–282**, 173 (2000).

[20] C. Moriyoshi, S. Shimomura, K. Itoh, K. Kojima, and K. Hiraoka, Crystal structure and valence transition temperature of YbInCu$_4$ single crystals, J. Magn. Magn. Mater. **260**, 206 (2003).

[21] V. N. Antonov, M. Galli, F. Marabelli, A. N. Yaresko, A. Ya. Perlov, and E. Bauer, Electronic structure and optical spectra of LuInCu$_4$ and YbMCu$_4$ (X = Cu, Ag, Au, Pd, and In), Phys. Rev. B **62**, 1742 (2000).

[22] V. N. Antonov, L. V. Bekenov, and A. N. Yaresko, Electronic structure of strongly correlated systems, Adv. Condens. Matter Phys. **2011**, 1 (2011).

[23] V. N. Antonov, L. V. Bekenov, and V. P. Antropov, Electronic structure and x-ray magnetic circular dichroism in YbAgCu$_4$ and YbInCu$_4$, Phys. Rev. B **89**, 165110 (2014).

[24] E. Figueroa, J. M. Lawrence, J. L. Sarrao, Z. Fisk, M. F. Hundley, and J. D. Thompson, Hall effect in YbXCu$_4$ and the role of carrier density in the YbInCu$_4$ valence transition, Solid State Commun. **106**, 347 (1998).

[25] I. Jarrige, A. Kotani, H. Yamaoka, N. Tsujii, K. Ishii, M. Upton, D. Casa, J. Kim, T. Gog, and J. N. Hancock, Kondo Interactions from Band Reconstruction in YbInCu$_4$, Phys. Rev. Lett. **114**, 126401 (2015).

[26] S. Ishihara, K. Ichiki, K. Abe, T. Matsumoto, K. Mimura, H. Sato, M. Arita, Eike F. Schwier, H. Iwasawa, K. Shimada, H. Namatame, M. Taniguchi, T. Zhuang, K. Hiraoka, and H. Anzai, The c-f hybridization effect in the subsurface region of YbInCu$_4$, J. Electron Spectrosc. Relat. Phenom. **220**, 66 (2017).

[27] J. W. Allen and R. M. Martin, α-γ transition in Ce. II. A detailed analysis of the Kondo volume-collapse model, Phys. Rev. B **46**, 5047 (1992).